Quantum interference between Zeeman levels near structures made of left-handed materials and matched zero-index metamaterials

Ge Song, Jingping Xu,* and Yaping Yang
MOE Key Laboratory of Advanced Micro-Structured Materials, School of Physics Science and Engineering, Tongji University, Shanghai 200092, People's Republic of China
(Received 16 November 2013; published 27 May 2014)

Quantum interference between Zeeman levels of atom placed in the structure containing left-handed materials (LHMs) and zero-index metamaterials (ZIMs) is investigated. Because of the existence of the LHM and ZIM, dipole radiation becomes highly anisotropic which is embodied by the high contrast between decay rates of the dipole component parallel to the surface and that normal to the surface. Furthermore, both decay rates are suppressed compared with those in free vacuum. Therefore, we propose the quantum interference between Zeeman levels accompanied by long lifetime. Two structures are designed to achieve such purpose. For the idealized LHM and ZIM without dissipation, a double-layer structure comprised of them is the right candidate. However, when we consider the dissipation of materials, a Fabry-Pérot cavity made of matched ZIM slabs and LHM slabs is required. Results show that we get a high degree of quantum interference and low decay rates simultaneously.

DOI: 10.1103/PhysRevA.89.053830 PACS number(s): 42.50.Gy, 32.60.+i, 42.50.Ct

I. INTRODUCTION

Quantum interference among different decay channels of a multilevel atomic system has attracted a lot of interest for a long time [1–10]; this can result in several fascinating phenomena, such as lasing without inversion [1,2], electromagnetically induced transparency [3,4], ultranarrow spectral line [5–7], and spontaneous emission cancellation [8]. However, strong quantum interference requires near-degenerate atomic transitions with near-parallel dipole moments sharing a common atomic state, which does not occur in real atoms [9]. For a V-type three-level atom, two upper Zeeman sublevels are $|1\rangle = |j = 1, m = 1\rangle$ and $|2\rangle = |j = 1, m = -1\rangle$, which can be made close to each other through Zeeman splitting, but the corresponding dipole moments are orthogonal to each other, in which one is left-rotation polarized and the other is right-rotation polarized. There is rarely experimental proof of strong quantum interference in natural atomic systems.

In 2000, Agarwal [11] pointed out that quantum interference between Zeeman levels can be revived in an anisotropic vacuum. The principle is that each transition dipole (left rotation or right rotation) can be redivided into two parts: one dipole component parallel to the surface and the other component normal to the surface. In anisotropic vacuum, radiation of the parallel component is suppressed while radiation of the normal component is enhanced or vice versa. Therefore the left-rotation and right-rotation dipoles are equivalent to the linear dipoles, which are effectively parallel to each other, and then quantum interference between them happens. Several anisotropic environments have been designed to revive the quantum interference between Zeeman levels [12–18], for example, placing the atom in photonic crystals [12,13], in the left-handed materials (LHMs) waveguide [14,15], near metal nanoshells [16], and near single negative metamaterials [17]. Furthermore, Yang *et al.* [18] introduced the concept of indirect quantum interference, and used a LHM slab to obtain strong quantum interference between Zeeman levels of atom at the position away from the surface according to the phase compensation and refocusing properties of LHM. However, it is difficult to totally suppress the decay of one component in reality, and previous studies [14–18] tried to enhance the decay of the other dipole component intensively through some special structures or metamaterials to achieve strong quantum interference. As a result, the enhanced decay rate becomes much higher [14,16,17], and the atomic lifetime becomes much shorter than that in vacuum, and so does the duration time of interference. An experimental observation of spontaneous emission cancellation in sodium dimers [19] has been performed but it could not be confirmed in a repetition of the experiment [20]. In an artificial quantum system, where levels of charged GaAs quantum dots can be designed by magnetic field and by doping, a spontaneously generated coherence arising from radiative decay has been observed [21]. This study is to find anisotropic environments for the atom with Zeeman levels theoretically, in which the dipole radiation is highly anisotropic but with suppressed decay rates compared to those in free vacuum. Therefore, an atom with Zeeman levels in it possesses strong quantum interference and long duration time of interference.

To construct such an environment, left-handed materials (LHMs) and zero-index metamaterials (ZIMs), both artificial microstructured materials, are required. LHM was first introduced by Veselago in 1968 [22], and refers to materials with negative permittivity, negative permeability, and negative refractive index simultaneously at interesting frequencies. LHM has recently attracted a lot of attention because of possible applications [23–26] and experimental demonstrations. Experimentally, LHM has been achieved over a wide range of frequencies, from the microwave up to the optical range [27–34]. The term "zero-index metamaterials" refers to the materials possessing effective zero refractive indexes, i.e., $\varepsilon = \mu = 0$ or $\varepsilon = 0, \mu \neq 0$ ($\varepsilon \neq 0, \mu = 0$). There are several approaches to achieve ZIM, e.g., embedding complementary metallic split-ring resonators in host media [35], exploiting the dispersion characteristics of composite metal-dielectric

*Corresponding author: xx_jj_pp@hotmail.com

waveguides [36,37], using composite right- or left-handed transmission lines [38,39], and designing metamaterials by stacking subwavelength structures such as thin layers [40]. Recently, effective zero refractive index at visible light frequency has been realized through a metal-insulator-metal waveguide at cutoff frequency [41] and a parallel array of subwavelength silver and silicon nitride nanolamellae [42]. Because of its unique electromagnetic properties, ZIM can be used to tailor the radiation phase patterns [43,44], squeeze electromagnetic waves [35,36,45], directional emission [46], cloaking [47], and Dirac-cone-like dispersions [48,49]. Though many structures are waveguides in experiments, here we suppose a bulk isotropic ZIM, which is characterized by $\varepsilon = \mu = 0$, and adopt its unique reflective behavior for oblique incidence [50]. The detailed discussion is presented in this context.

This paper is organized as follows. In Sec. II, we describe our model and give the principle of reviving the quantum interference between Zeeman levels of atom in an anisotropic vacuum. In Sec. III, we discuss the quantum interference between Zeeman levels of atom in the structures made of LHM and matched ZIM. Two kinds of structures are designed, i.e., double-layer structure and Fabry-Pérot cavity. They can generate both strong quantum interference and lower decay rates in the case of lossless and dissipation, correspondingly. Finally we present our conclusions in Sec. IV.

II. QUANTUM INTERFERENCE OF A ZEEMAN THREE-LEVEL ATOM

Figure 1(a) depicts the energy scheme of a V-type three-level atom. Two upper levels are Zeeman sublevels $|1\rangle = |j = 1, m = 1\rangle$ with energy $\hbar\omega_1$ and $|2\rangle = |j = 1, m = -1\rangle$ with energy $\hbar\omega_2$. The ground state is $|3\rangle = |j = 0, m = 0\rangle$ with energy equal to zero. The y direction is chosen as the quantization axis (i.e., by applying a static magnetic field along the y direction), and it leads to the Zeeman split. In the present work, the V-type three-level atom is placed on the left of a structure made of a LHM slab mounted on a matched ZIM slab as shown in Fig. 1(b). Both the left and right sides of the double-layer structure are vacuums. The thicknesses of LHM and matched ZIM slabs are d_1 and d_2, respectively. The left interface of the structure is taken as the origin of the z coordinate. The atomic dipole moment operator can be described as $\boldsymbol{d} = d(A_{13}\boldsymbol{e}_l + A_{23}\boldsymbol{e}_r) + \text{H.c.}$, where $A_{ij} = |i\rangle\langle j|$ $(i, j = 1,2,3)$ is the atomic transition operator. $\boldsymbol{e}_r = (\boldsymbol{e}_z + i\boldsymbol{e}_x)/\sqrt{2}$ and $\boldsymbol{e}_l = (\boldsymbol{e}_z - i\boldsymbol{e}_x)/\sqrt{2}$ refer to right-rotating and left-rotating unit vectors, respectively. The amplitude of the dipole moment d is chosen to be real.

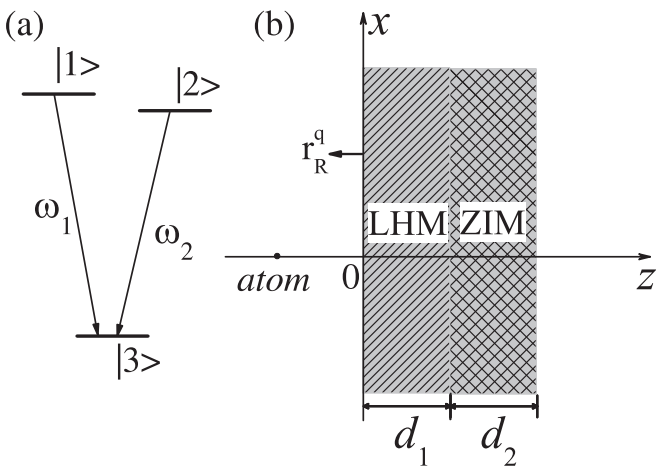

FIG. 1. (a) The energy scheme of the atom; (b) the V-type three-level atom is placed near the structure made of LHM and matched ZIM.

The simultaneous equations of the expectation values of atomic operators for the V-type three-level atom are [13]

$$\frac{d}{dt}\langle A_{11}\rangle = -2\gamma_1\langle A_{11}\rangle - \kappa_2\langle A_{12}\rangle - \kappa_2\langle A_{21}\rangle, \tag{1}$$

$$\frac{d}{dt}\langle A_{22}\rangle = -2\gamma_2\langle A_{22}\rangle - \kappa_1\langle A_{21}\rangle - \kappa_1\langle A_{12}\rangle, \tag{2}$$

$$\frac{d}{dt}\langle A_{12}\rangle = -[\gamma_1 + \gamma_2 + i(\omega_2 - \omega_1)]\langle A_{12}\rangle - \kappa_1\langle A_{11}\rangle - \kappa_2\langle A_{22}\rangle. \tag{3}$$

Here γ_1 and γ_2 are the spontaneous decay rates of transition channels $|1\rangle \to |3\rangle$ and $|2\rangle \to |3\rangle$, respectively. κ_1 and κ_2 are the quantum interference between two decay channels. It is shown that due to κ_1 and κ_2, the exceptive value of atomic operators $\langle A_{11}\rangle$, $\langle A_{22}\rangle$, and $\langle A_{12}\rangle$ relates to each other during evolution.

With the two Zeeman upper levels nearly degenerated, the approximation $\omega_1 \approx \omega_2 = \omega_0$ is reasonable. Therefore we have $\gamma_1 = \gamma_2 = \gamma$ and $\kappa_1 = \kappa_2 = \kappa$, which are expressed as

$$\begin{aligned}\gamma_1 = \gamma_2 = \gamma &= d^2\omega_0^2\boldsymbol{e}_l \cdot \text{Im}\boldsymbol{G}(z_1, z_1, \omega_0) \cdot \boldsymbol{e}_r \\ &= d^2\omega_0^2\text{Im}[G_{zz}(z_1, z_1, \omega_0) + G_{xx}(z_1, z_1, \omega_0)]/2,\end{aligned} \tag{4}$$

$$\begin{aligned}\kappa_1 = \kappa_2 = \kappa &= d^2\omega_0^2\boldsymbol{e}_l \cdot \text{Im}\boldsymbol{G}(z_1, z_1, \omega_0) \cdot \boldsymbol{e}_l \\ &= d^2\omega_0^2\text{Im}[G_{zz}(z_1, z_1, \omega_0) - G_{xx}(z_1, z_1, \omega_0)]/2.\end{aligned} \tag{5}$$

The relative strength of quantum interference $p = \kappa/\sqrt{\gamma_1\gamma_2}$ [13] is used to measure quantum interference. With the definition of $\Gamma_\perp = d^2\omega_0^2\text{Im}G_{zz}(z_1, z_1, \omega_0)$ and $\Gamma_{||} = d^2\omega_0^2\text{Im}G_{xx}(z_1, z_1, \omega_0)$, we can get $\gamma = (\Gamma_\perp + \Gamma_{||})/2$, $\kappa = (\Gamma_\perp - \Gamma_{||})/2$, and

$$p = \frac{\Gamma_\perp - \Gamma_{||}}{\Gamma_\perp + \Gamma_{||}}. \tag{6}$$

Here $\Gamma_\perp$ and $\Gamma_{||}$ are the spontaneous decay rates of the dipole component perpendicular to the interface (along the z axis) and parallel to the interface (along the x axis), respectively. In a free vacuum or isotropic environment, $\Gamma_\perp = \Gamma_{||}$ and $\kappa = 0$; therefore quantum interference disappears. However, if the vacuum is anisotropic, which means $G_{zz} \neq G_{xx}$ and $\Gamma_\perp \neq \Gamma_{||}$, $\kappa \neq 0$ and the quantum interference will present. Obviously, p increases with the difference between $\Gamma_\perp$ and $\Gamma_{||}$. If $\Gamma_{||} = 0$ or $\Gamma_\perp = 0$, then $p = \pm 1$, γ_1 and γ_2 are parallel to each other equivalently, and the complete quantum interference happens. If $\Gamma_\perp$ or $\Gamma_{||}$ cannot be suppressed deeply, the condition $\Gamma_\perp \gg \Gamma_{||}$ or $\Gamma_{||} \gg \Gamma_\perp$ can still approach $p = \pm 1$. With $p \neq 0$ in hand, plenty of quantum interference phenomena can be realized with different initial conditions.

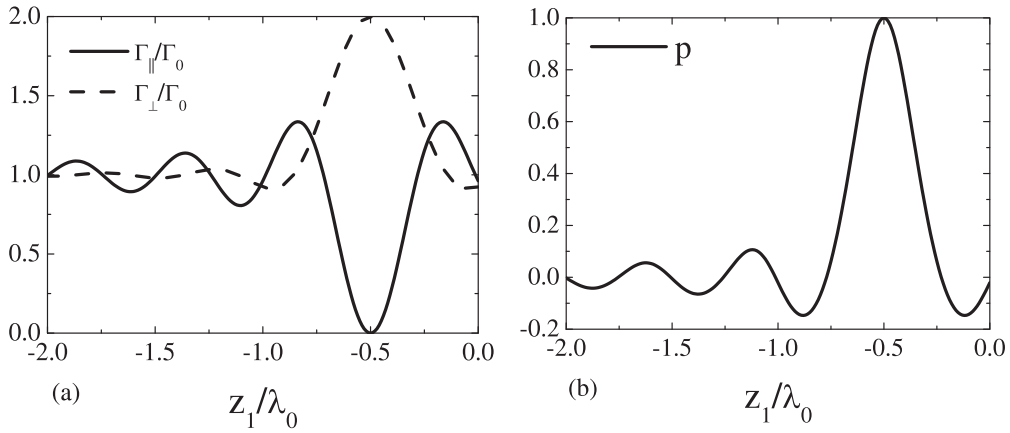

FIG. 2. (a) The decay rates and (b) the relative strength of the quantum interference p as a function of atomic position when the atom is placed near the LHM slab mounted on an ideal metal mirror. The thickness of the LHM slab is $d_1 = 0.5\lambda_0$, $\varepsilon_{\rm LHM} = \mu_{\rm LHM} = -1$, $r^{TE}_{\rm mirr} = -1$, and $r^{TM}_{\rm mirr} = 1$.

With the help of Green's tensor in a multilayer [51], the decay rates $\Gamma_\perp$ and $\Gamma_{||}$ can be expressed as

$$\Gamma_\perp = \frac{3}{2}\Gamma_0 \mathrm{Re}\left(\int_0^{K_0} + \int_{K_0}^{\infty}\right)\frac{dK_{||}}{K_{0z}}\frac{K_{||}^3}{K_0^3}\left[1 + r_R^{\rm TM} e^{-2iK_{0z}z_1}\right] = \Gamma_{\perp\rm rad} + \Gamma_{\perp\rm nonrad}, \quad (7)$$

$$\Gamma_{||} = \frac{3}{4}\Gamma_0 \mathrm{Re}\left(\int_0^{K_0} + \int_{K_0}^{\infty}\right)\frac{dK_{||}}{K_0}\frac{K_{||}}{K_{0z}}\left[\left(1 + r_R^{\rm TE} e^{-2iK_{0z}z_1}\right) + \frac{K_z^2}{K_0^2}\left(1 - r_R^{\rm TM} e^{-2iK_{0z}z_1}\right)\right] = \Gamma_{||\rm rad} + \Gamma_{||\rm nonrad}. \quad (8)$$

Here $K_0 = \omega_0/c$ is the wave number in vacuum. K_{0z} is the z component of the wave vector, while $K_{||}$ is the projection of the wave vector on the x-y plane. They satisfy the relationship of $K_{||}^2 + K_{0z}^2 = K_0^2$. $\Gamma_0 = d^2\omega_0^3/(3\pi\varepsilon_0\hbar c^3)$ is the decay rate of dipole moment d with transition frequency ω_0 in free vacuum, and is the reference of the decay rate. r_R^q is the reflective coefficient of the right surrounding area of an atom for polarization $q = \mathrm{TE}$ or TM, which can be gotten by using the multiple-beam interference method [52]. In Eqs. (7) and (8), decay rates are divided into two parts: the radiative decay rate and nonradiative rate. Radiative decay refers to the decay occurring through emitting a propagating photon while nonradiative decay originates from a Coulomb interaction between the atom and surrounding area which happens only near the surrounding area containing dissipation. In the usual case, nonradiative decay is dominant for an atom close to the surface, while radiative decay is dominant for an atom far away from the surface.

III. QUANTUM INTERFERENCE OF A ZEEMAN ATOM NEAR THE STRUCTURE CONTAINING MATCHED ZIM

It is well known that atomic spontaneous decay near a metal mirror is anisotropic. Agarwal [11] showed that an atom with Zeeman levels located on the surface of an ideal metal mirror possesses $\Gamma_{||} = 0$, $\Gamma_\perp = 2\Gamma_0$, and $p = 1$; therefore quantum interference is revived. The anisotropy originates from the boundary condition of the electromagnetic wave at an ideal metal surface, i.e., $r^{\rm TE}_{\rm mirr} = -1$ and $r^{\rm TM}_{\rm mirr} = 1$. Xu and Yang [15] introduced the ideal LHM ($\varepsilon_{\rm LHM} = \mu_{\rm LHM} = -1$) slab mounted on an ideal metal mirror to get complete quantum interference over a macroscopic distance. Decay rates and relative strength of quantum interference as a function of atomic position in such a structure are plotted in Fig. 2.

From Fig. 2, it is clear that, for the atom near the LHM slab mounted on an ideal metal mirror, the high anisotropic position with $\Gamma_{||} = 0$ and $\Gamma_\perp = 2\Gamma_0$ has been moved to the position of $z_1 = -d_1 = -0.5\lambda_0$, and complete quantum interference between Zeeman levels happens with $p = 1$. Away from this position, p decreases with oscillation and tends to 0. In the view of transformation optics [23,25], the parameters of a LHM slab are set as $\varepsilon_{\rm LHM} = -1$ and $\mu_{\rm LHM} = -1$ in order to optically cancel the vacuum with the same thickness ($d_1 = d_{\rm vacuum}$) between the atom and the structure; then the atom is just placed on the surface of the ideal mirror. Therefore, the high anisotropic point has been transformed to the position $z_1 = -d_1 = -0.5\lambda_0$ due to the ideal LHM. It is obvious that this transformation always exists and is independent of the thickness of the ideal LHM. In other words, the reflective coefficients of such structure are $r_R^{\rm TE} = -e^{-2iK_{0z}d_1}$ and $r_R^{\rm TM} = e^{-2iK_{0z}d_1}$ due to the phase compensation and refocusing properties of LHM [18]. From Eqs. (7) and (8) we can get $\Gamma_\perp = 3\Gamma_0 \mathrm{Re}\int_0^{K_0} dK_{||}K_{||}^3 K_{0z}^{-1}K_0^{-3}$ and $\Gamma_{||} = 0$ when the atom is located at $z_1 = -d_1$. After simple deduction $\Gamma_\perp = 2\Gamma_0$ will emerge at $z_1 = -d_1$. Therefore complete quantum interference will always occur at the position $z_1 = -d_1$ for such ideal structure. The advantages of such design are to realize the strong quantum interference away from the surface and weaken the influence of the material's dissipation, because the corresponding nonradiative decay is dominant near the surface. Although such structure can approach complete quantum interference, the decay rate of the dipole component perpendicular to the surface is enhanced to twice the decay rate in free vacuum, i.e., $\Gamma_\perp = 2\Gamma_0$.

Obviously, electromagnetic characters play an important role in anisotropy and quantum interference. For a bulk matched ZIM, i.e., $\varepsilon_{\rm ZIM} = \mu_{\rm ZIM} = 0$ and $n_{\rm ZIM} = 0$, when an electromagnetic wave is incident from vacuum to the

ZIM, the critical angle θ_1 is zero and oblique incidence causes total reflection based on Snell's law. Specifically, the reflective coefficient for TM (TE) wave at oblique incidence is $r^{\mathrm{TM}}_{\mathrm{interface}} \to -1$ ($r^{\mathrm{TE}}_{\mathrm{interface}} \to -1$) according to the Fresnel formula, i.e., the limitation of $r^{\mathrm{TM}}_{\mathrm{interface}} = (\varepsilon_2 k_{1z} - \varepsilon_1 k_{2z})/(\varepsilon_2 k_{1z} + \varepsilon_1 k_{2z})$ ($r^{\mathrm{TE}}_{\mathrm{interface}} = (\mu_2 k_{1z} - \mu_1 k_{2z})/(\mu_2 k_{1z} + \mu_1 k_{2z})$) with $\varepsilon_2 = \varepsilon_{\mathrm{ZIM}} \to 0$ ($\mu_2 = \mu_{\mathrm{ZIM}} \to 0$). For a matched ZIM slab with thickness d_2 in vacuum, the reflective coefficient can be expressed as

$$r^{\mathrm{TE/TM}}_{\mathrm{ZIM\text{-}slab}} = \frac{r^{\mathrm{TE/TM}}_{\mathrm{interface}} - r^{\mathrm{TE/TM}}_{\mathrm{interface}} e^{2ik_{2z}d_2}}{1 - \left(r^{\mathrm{TE/TM}}_{\mathrm{interface}}\right)^2 e^{2ik_{2z}d_2}}. \tag{9}$$

It is easy to get $r^{\mathrm{TE/TM}}_{\mathrm{ZIM\text{-}slab}} = -1$ at oblique incidence and this value is independent on the thickness d_2. In other words, the matched ZIM slab allows transmittance only at normal incidence but reflects all light at oblique incidence [50]. Though the ZIM is transparent for normal incident, it can be seen as total reflection here because the atomic decay covers all directional radiation. This is the key difference of a matched ZIM compared to an ideal metal, since the reflective coefficient for TM incident at the ideal metal is $r^{\mathrm{TM}}_{\mathrm{mirr}} = 1$. In the following we will show results of strong quantum interference with suppressed decay rates by using the unique reflective character of ZIM.

A. Structure without dissipation

We consider the structure of Fig. 1 without losses, in which layer 1 is the ideal LHM slab with $\varepsilon_{\mathrm{LHM}} = \mu_{\mathrm{LHM}} = -1$ while layer 2 is the ideal matched ZIM slab with $\varepsilon_{\mathrm{ZIM}} = \mu_{\mathrm{ZIM}} = 0$. The thickness of the ideal LHM determines only the position of strong quantum interference and does not contribute to the decay rates. For simplicity we suppose the same thicknesses for layers (i.e., $d_1 = d_2 = 0.5\lambda_0$), and the influence of the thickness will be presented later. The decay rates of two dipole orientations and p as a function of atom position are given in Fig. 3. As discussed above, the reflective coefficients in Eqs. (7) and (8) become $r^{\mathrm{TE}}_R = -e^{-2iK_{0z}d_1}$ and $r^{\mathrm{TM}}_R = -e^{-2iK_{0z}d_1}$ here, where the phase compensation of LHM is still working. It is clear from Fig. 3 that the complete quantum interference $p = -1$ is still happening at the position of $z_1 = -d_1 = -0.5\lambda_0$. However, there are two differences from the material containing metal of Fig. 2. The first, $\Gamma_{||}$ and $\Gamma_\perp$ in Fig. 3 are suppressed simultaneously near the focus point $z_1 = -0.5\lambda_0$, i.e., $\Gamma_{||} = 0.5\Gamma_0$ while $\Gamma_\perp = 0$. It is easy to understand according to Eqs. (7) and (8). For $\Gamma_\perp$ of Eq. (7), the integrated band is zero at $z_1 = -d_1$ when substituting $r^{\mathrm{TM}}_R = -e^{-2iK_{0z}d_1}$ into it; therefore $\Gamma_\perp = 0$ at this position. For $\Gamma_{||}$ at $z_1 = -d_1$, Eq. (8) becomes $\Gamma_{||} = (3/2)\Gamma_0 \mathrm{Re}\int_0^K dK_{||} K_{||} K_z K^{-3}$ by inserting $r^{\mathrm{TE}}_R = -e^{-2iK_{0z}d_1}$ and $r^{\mathrm{TM}}_R = -e^{-2iK_{0z}d_1}$ into it, and finally we get $\Gamma_{\|} = 0.5\Gamma_0$ after simple deduction. The second difference from metal is that away from the focus point, the decay rate has weaker amplitude of oscillation, and it can approach the decay rate in free space Γ_0 quickly. This also originates from $r^{\mathrm{TM}}_R = -e^{-2iK_{0z}d_1}$.

Therefore, by replacing the ideal metal by ZIM, an atom near the structure of Fig. 1 can approach complete quantum interference of $p = -1$ with suppressed decay rate as $\Gamma_{||} = 0.5\Gamma_0$ while $\Gamma_\perp = 0$ at the position of $z_1 = -d_1 = -0.5\lambda_0$. In previous works, the authors got strong quantum interference by enhancing either $\Gamma_{||}$ or $\Gamma_\perp$ to hundreds of times that in free vacuum, i.e., $\Gamma_\perp \approx 10^4\Gamma_0$ [14], $\Gamma_\perp \approx 60\Gamma_0$ [16], and $\Gamma_{||} \approx 50\Gamma_0$ [17]. Consequently, the atomic lifetime as well as the duration of interference is decreased. In our system, strong quantum interference is accompanied by suppressed decay rates; as a result, the atomic lifetime is prolonged and so is the time of interference. This is quite useful to keep quantum interference for a long time.

The influence of thicknesses has been shown in Fig. 4. Here the thicknesses of LHM and ZIM slabs are $d_1 = 2\lambda_0$ and $d_2 = 3\lambda_0$. It indicates the same behavior in Fig. 3, i.e.; complete quantum interference occurs at position $z_1 = -d_1$, decay is suppressed, and oscillation behaviors are the same. Due to the focusing and phase compensation effects of LHM, with the increasing of LHM slab's thickness d_1, the position possessing strong quantum interference will shift away from the structure, and its coordinate is $z_1 = -d_1$. Meanwhile, as mentioned in the beginning of Sec. III, the reflective character of a matched ZIM slab is independent of thickness. Therefore, without losses neither the thickness of LHM nor the thickness of matched ZIM could affect the behavior of atomic decay in our structure, as shown in Fig. 4.

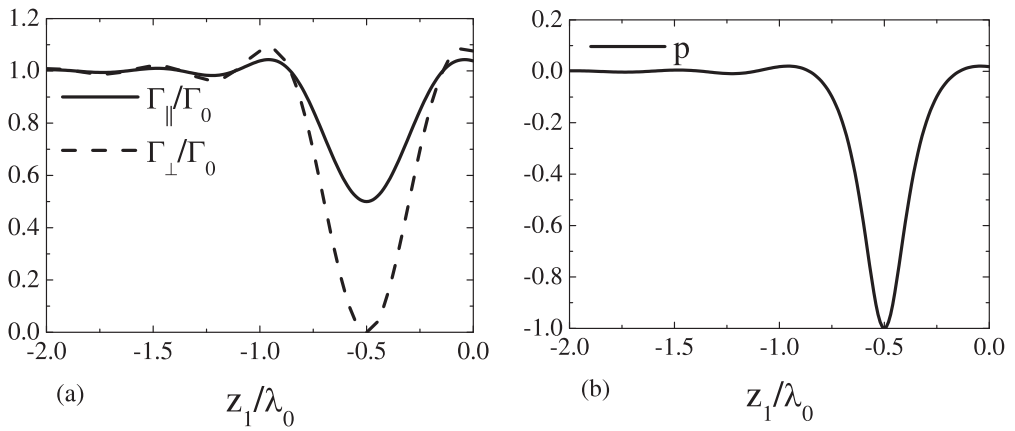

FIG. 3. (a) The decay rates and (b) p as a function of z_1. The thicknesses of LHM and matched ZIM slabs are $d_1 = d_2 = 0.5\lambda_0$. $\varepsilon_{\mathrm{LHM}} = \mu_{\mathrm{LHM}} = -1$ and $\varepsilon_{\mathrm{ZIM}} = \mu_{\mathrm{ZIM}} = 0$.

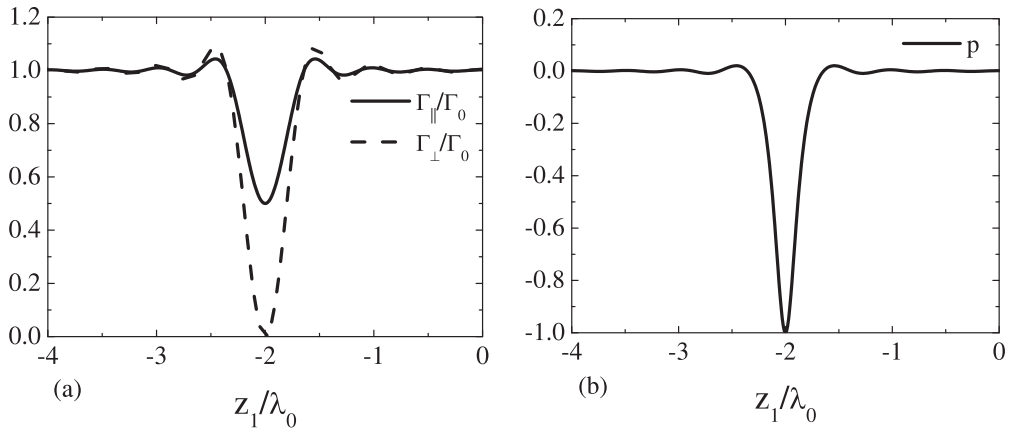

FIG. 4. (a) The decay rates and (b) p as a function of z_1 with $d_1 = 2\lambda_0$ and $d_2 = 3\lambda_0$. Other parameters are the same as in Fig. 3.

B. Structure with dissipation

According to the Kramers-Kronig relation, there is inevitable dissipation in reality materials. The influence of the LHM's and ZIM's dissipation on quantum interference must be taken into account. We set $\varepsilon_{\rm LHM}(\omega_0) = \mu_{\rm LHM}(\omega_0) = -0.99 + i0.003$ and $\varepsilon_{\rm ZIM}(\omega_0) = \mu_{\rm ZIM}(\omega_0) = 0.001 + i0.003$. Therefore, the real part of LHM's refractive index is near -1 and that of ZIM's refractive index is 0.001. Their imaginary parts are small at the atomic transition frequency ω_0. With Eqs. (6)–(8), we plot $\Gamma_\perp$, $\Gamma_{||}$, and p as a function of atomic position in Fig. 5.

From the solid curves in Figs. 5(a) and 5(b), at the focus position of $z_1 = -0.5\lambda_0$, $\Gamma_{||}$ deviates from $0.5\Gamma_0$ while $\Gamma_\perp$ deviates from 0. The reason is mainly the nonradiative decay due to dissipation. According to Eqs. (7) and (8), such nonradiative decay rates can be distinguished and are shown by the dotted lines in Fig. 5. When an atom is near the interface ($|z_1| < 0.2\lambda_0$), the contribution of the nonradiative decay is dominating and it decreases rapidly with increasing distance $|z_1|$. Without the LHM slab, the anisotropic space only occurs near the interface, and it will be destroyed drastically by the huge nonradiative decay in case of dissipation. With the benefit of the LHM slab, the position of strong quantum interference has been moved and the influence of nonradiative decay has been weakened. This is the reason of using a LHM slab. Besides, it is very difficult to fabricate metamaterials with $\varepsilon,\mu = -1$ (0) [32,42], so these parameters are chosen with a little deviation from ideal values. As a result, the value of strong quantum interference shifts to -0.58 as shown in Fig. 5(c). Although a LHM slab can weaken the influence of nonradiative decay here, the relative strength of quantum interference apparently decreases compared with previous results [15,17]. The reason is that both $\Gamma_{||}$ and $\Gamma_\perp$ are suppressed, and it is hard to increase their contrast.

If we further increase the loss of ZIM, the relative strength of quantum interference will be decreased correspondingly. The index of ZIM is chosen as $\varepsilon_{\rm ZIM}(\omega_0) = \mu_{\rm ZIM}(\omega_0) = 0.001 + ix$. In Fig. 6, we plot $\Gamma_\perp$, $\Gamma_{||}$, and p values as a function of z_1 in the structure of Fig. 1 with a different imaginary part of ZIM's indexes.

From Fig. 6, for $x = 0.09$, although both decay rates are still suppressed, p shifts to -0.4 at $z_1 = -0.53\lambda_0$ and the strength of quantum interference decreases. Therefore, to obtain strong strength of quantum interference with suppressed decay rate in the case of loss, we need to design another Structure.

C. Fabry-Pérot cavity made of LHM and ZIM

Several structures were suggested to get strong quantum interference considering the dissipation of materials, such as negative-refractive-index waveguide [14], Fabry-Pérot cavity filled with LHM by half [15], metal nanoshells [16], and

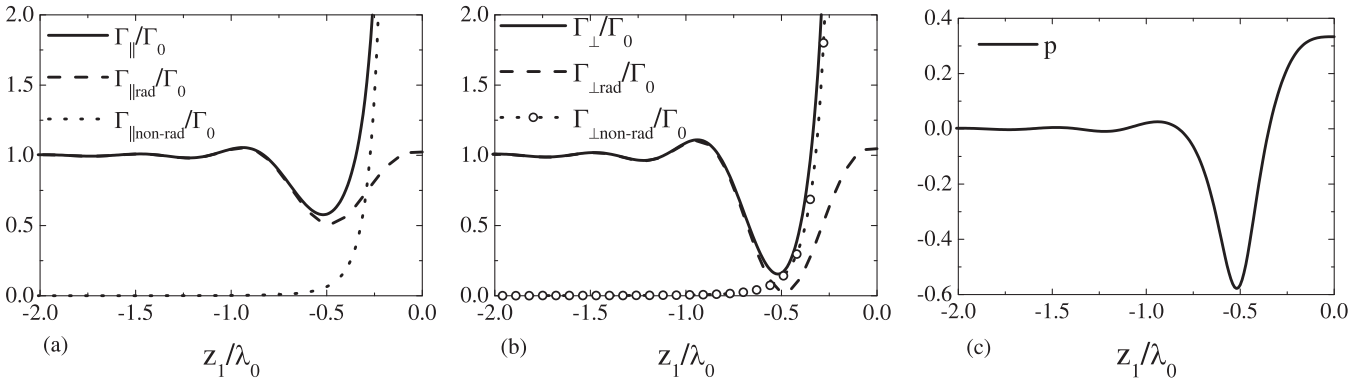

FIG. 5. (a) $\Gamma_{||}$, (b) $\Gamma_\perp$, and (c) p as a function of z_1. The thicknesses of LHM and ZIM slabs are $d_1 = d_2 = 0.5\lambda_0$. $\varepsilon_{\rm LHM}(\omega_0) = \mu_{\rm LHM}(\omega_0) = -0.99 + i0.003$ and $\varepsilon_{\rm ZIM}(\omega_0) = \mu_{\rm ZIM}(\omega_0) = 0.001 + i0.003$.

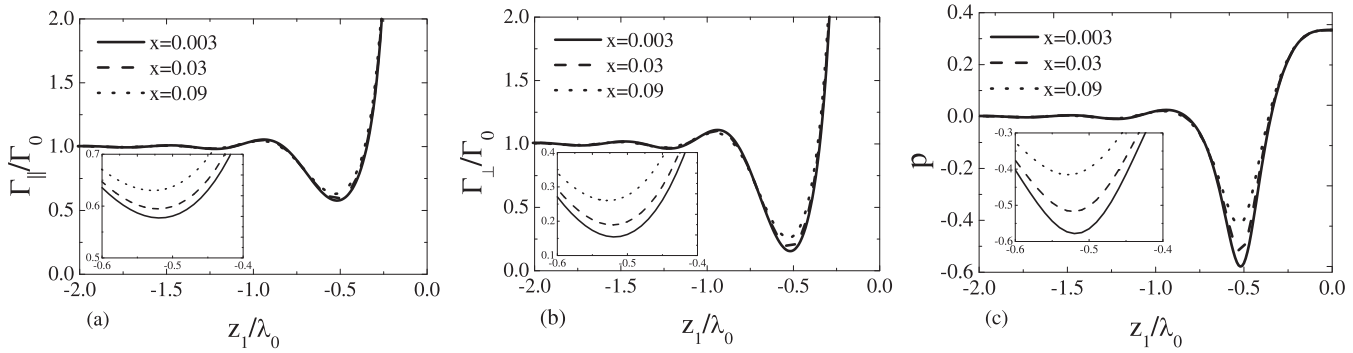

FIG. 6. (a) $\Gamma_{||}$, (b) $\Gamma_\perp$, and (c) p as a function of z_1 with $\varepsilon_{\rm ZIM}(\omega_0) = \mu_{\rm ZIM}(\omega_0) = 0.001 + ix$, and other parameters are the same as Fig. 5. Insets: Magnification of the region with z_1 from $-0.6\lambda_0$ to $-0.4\lambda_0$.

μ-negative slab [17]. Enlightened by previous works [15,18], we still construct a Fabry-Pérot cavity but the mirror of the cavity is composed of a LHM slab mounted on a ZIM, as shown in Fig. 7. Here the thickness of the middle vacuum is twice as long as that of the LHM slab, and the atom is placed in the center.

In this structure, decay rates of perpendicular and parallel dipoles should be modified as

$$\Gamma_\perp = \frac{3}{2}\Gamma_0 \mathrm{Re}\int_0^\infty \frac{dK_{||}}{K_{0z}}\frac{K_{||}^3}{K_0^3}\left[1 + \frac{2r_L^{\rm TM}r_R^{\rm TM}e^{2iK_{0z}d_0} + r_L^{\rm TM}e^{2iK_{0z}(d_0+z_1)} + r_R^{\rm TM}e^{-2iK_{0z}z_1}}{D_{\rm TM}}\right], \tag{10}$$

$$\Gamma_{||} = \frac{3}{4}\Gamma_0 \mathrm{Re}\int_0^\infty \frac{dK_{||}}{K_0}\frac{K_{||}}{K_{0z}}\left\{\left[1 + \frac{2r_L^{\rm TE}r_R^{\rm TE}e^{2iK_{0z}d_0} + r_L^{\rm TE}e^{2iK_{0z}(d_0+z_1)} + r_R^{\rm TE}e^{-2iK_{0z}z_1}}{D_{\rm TE}}\right]\right.$$
$$\left. + \frac{K_{0z}^2}{K_0^2}\left[1 + \frac{2r_L^{\rm TM}r_R^{\rm TM}e^{2iK_{0z}d_0} - r_L^{\rm TM}e^{2iK_{0z}(d_0+z_1)} - r_R^{\rm TM}e^{-2iK_{0z}z_1}}{D_{\rm TM}}\right]\right\}. \tag{11}$$

The reflective coefficient of the left surrounding area of atom r_L^q has to be considered here. $D_q = 1 - r_L^q r_R^q e^{2ik_{0z}d_0}$ originates from the multireflection in cavity.

The indexes of LHM and ZIM are set to be $\varepsilon_{\rm LHM} = \mu_{\rm LHM} = -0.99 + i0.003$ and $\varepsilon_{\rm ZIM} = \mu_{\rm ZIM} = 0.001 + ix$. In Fig. 8, we calculate $\Gamma_{||}$, $\Gamma_\perp$, and p as a function of z_1 with the structure parameters $d_1 = d_2 = 0.5\lambda_0$ and $x = 0.03$.

From Fig. 8(c), the strength of quantum interference is improved ($p \approx -0.9$) at position $z_1 = -0.5\lambda_0$. Comparing with Fig. 6(c), in which the strength of quantum interference is about -0.5, the structure in Fig. 7 indeed enhances quantum interference. The influence of nonradiative decay related to the material's loss has been attenuated due to its being a half wavelength away from the surface [dotted curves in Figs. 8(a) and 8(b)]. Such high degree of quantum interference mainly comes from the high contrast of radiative decays [dashed curves in Figs. 8(a) and 8(b)], since at $z_1 = -0.5\lambda_0$ the radiative decay rate of a normal dipole is suppressed deeply, while radiative decay of a parallel dipole is enhanced to $2.2\Gamma_0$ due to the resonance of the cavity. Such high contrast of decay rates originates from the collective work of LHM, ZIM, and the cavity. The cavity of Fig. 7 can be equivalent to be the cavity made of ZIM with zero effective thickness due to phase compensation of LHM slabs. The decay of a normal dipole is still suppressed to 0 due to ZIM, but decay of a parallel dipole is enhanced due to the resonance of the cavity.

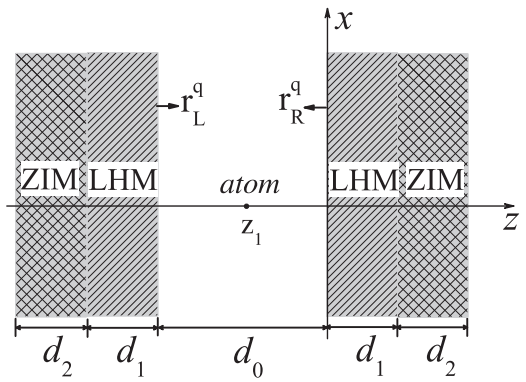

FIG. 7. The scheme of a Fabry-Pérot cavity made of LHM and ZIM.

In the case of Fig. 8, though radiative decay rates show high anisotropy with $p = -0.9$ at position $z_1 = -0.5\lambda_0$, the decay rate of the parallel dipole is still enhanced, about $\Gamma_{||} = 2.5\Gamma_0$. As usual, when a dipole is near the material with dissipation, high p is accompanied by enhanced decay of one component; for example, the decay rate is larger than $3\Gamma_0$ in a specific negative-refractive-index waveguide [14], $\Gamma_\perp > 3\Gamma_0$ in a Fabry-Pérot cavity filled with LHM by half [15], $\Gamma_\perp \approx 60\Gamma_0$ near an absorbing metal surface [16], and $\Gamma_{||}$ is on the order of $10^2\Gamma_0$ near the μ-negative slab [17]. However, the rates will be attenuated with the increasing of the thickness of the cavity here due to the influence of dissipation. Therefore $\Gamma_{||}$ will decrease with the increasing of d_0, but the suppression of

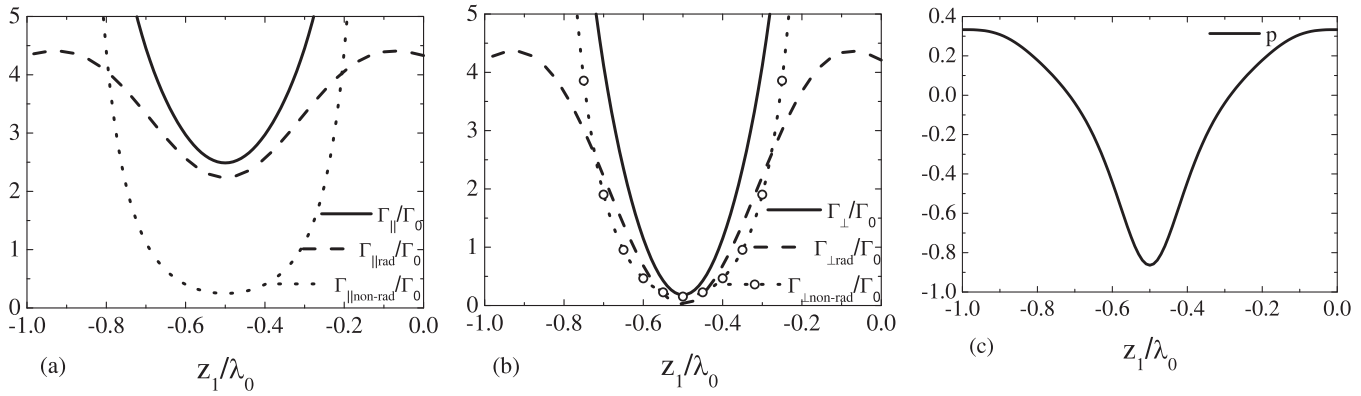

FIG. 8. (a) $\Gamma_{||}$, (b) $\Gamma_{\perp}$, and (c) p as a function of z_1. The thicknesses are $d_1 = d_2 = 0.5\lambda_0$ and $d_0 = 2d_1$. Other parameters are $\varepsilon_{\rm LHM}(\omega_0) = \mu_{\rm LHM}(\omega_0) = -0.99 + i0.003$ and $\varepsilon_{\rm ZIM}(\omega_0) = \mu_{\rm ZIM}(\omega_0) = 0.001 + i0.03$.

$\Gamma_{\perp}$ is relatively insensitive to it. Therefore, choosing suitable d_0, we would get the high p with lower decay rates. In Fig. 9, we plot $\Gamma_{||}$, $\Gamma_{\perp}$, and p as a function of d_0 with structure parameters $z_1 = -d_1$ and $d_0 = 2d_1$.

It is clear from Fig. 9, that with the increasing of d_0, both $\Gamma_{||}$ and $\Gamma_{\perp}$ are smaller than Γ_0 when $d_0 > 2\lambda_0$. In our structure, radiative decay of a dipole normal to the surface decreases with distance much more sharply than that of a dipole parallel to the surface and it is nearly suppressed completely in an appropriate range. Meanwhile, decay of a dipole parallel to the surface is a little smaller than Γ_0. Such different behavior of decays can produce strong quantum interference with suppressed decay rates by adopting appropriate thickness of cavity. It is clear that in the range of $2\lambda_0 < d_0 < 4\lambda_0$, dipole decays show high anisotropy with $|p| > 0.7$ even if the dissipation $x = 0.09$, which is shown in Fig. 9(c). High p and low decays have been attributed to the function of the ZIM slab, which could suppress decay rates of both dipole orientations. Previous discussion focused on the case that the real part of $\varepsilon_{\rm ZIM}$ and $\mu_{\rm ZIM}$ is 0.001, which is a little difficult in experiment. However, we find the degree of quantum interference is acceptable even if the real part of $\varepsilon_{\rm ZIM}$ and $\mu_{\rm ZIM}$ approaches 0.1 under appropriate conditions, which reduces the technical requirements of the experiment. In Fig. 9(d), we plot p as a function of both the real part and the imaginary part of $\varepsilon_{\rm ZIM}$ with $\mu_{\rm ZIM} = \varepsilon_{\rm ZIM}$, $d_0 = 2\lambda_0$, and $z_1 = -d_0/2$. It is clear that $|p|$ decreases with the increasing of Re($\varepsilon_{\rm ZIM}$) in general. However, $|p|$ still reaches 0.73 even if Re($\varepsilon_{\rm ZIM}$) is about 0.01 for appropriate

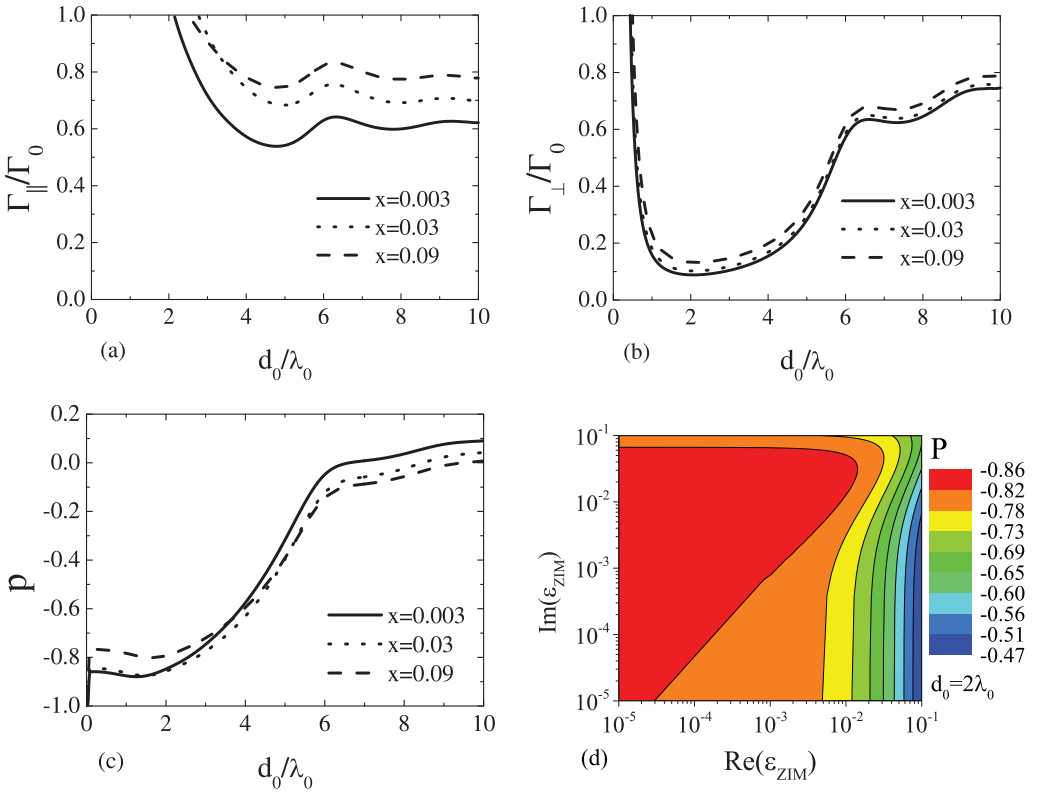

FIG. 9. (Color online) (a) $\Gamma_{||}$, (b) $\Gamma_{\perp}$, and (c) p as a function of d_0 with $d_0 = 2d_1 = -2z_1$, $\varepsilon_{\rm ZIM}(\omega_0) = \mu_{\rm ZIM}(\omega_0) = 0.001 + ix$. (d) p as a function of Re($\varepsilon_{\rm ZIM}$) and $Im(\varepsilon_{\rm ZIM})$ when $\varepsilon_{\rm ZIM} = \mu_{\rm ZIM}$ and $d_0 = 2\lambda_0$. Other parameters are the same as in Fig. 8.

dissipation. When $\mathrm{Re}(\varepsilon_{\mathrm{ZIM}})$ is about 0.1, $|p|$ is around 0.5. Therefore, through introducing ZIM to suppress the decay, our model can hold a high p and low decays (increased duration time of interference) simultaneously.

D. Discussion

Our results indicate an attractive implementation of quantum interference in atomic or molecular systems by using LHM and ZIM slabs. Many applications related to quantum interference have been suggested in the literature [9,10] but without clear experimental implementation. Since the duration time of interference is increased in our structure, it will be convenient to measure this quantum effect in experiment. So far, LHM has reached telecommunication [28–32] and visible wavelengths [33,34]. LHM around the wavelength of 780 nm has been demonstrated with $\mathrm{Re}(n) \approx -0.6$ by using a Ag-MgF_2-Ag fishnet structure [34]. Furthermore, three-dimensional LHM made of cascaded fishnet metamaterials shows a refractive index of $\mathrm{Re}(n) \approx -1$ at a wavelength of 1.7 μm and experimental results serve as direct evidence of zero and negative phase index in the metamaterial [32]. In those experiments, a refractive index of $\mathrm{Re}(n) \approx 0$ was also achieved at a certain wavelength. In a recent experiment, an epsilon-near-zero metamaterial composed of a carefully sculpted parallel array of subwavelength silver and silicon nitride nanolamellae shows a vanishing effective permittivity at visible wavelengths [42]. However, for our work to lead to applications, several goals need to be achieved: LHM and ZIM at the same operation wavelength, both epsilon- and mu-near-zero metamaterial, and reduction of losses. These challenges could be overcome with rational design and nanoscale fabrication. In a recent work, a single-layer wide-angle negative-index metamaterial, consisting of a hexagonal close-packed array of Ag-GaP-Ag coaxial waveguides, has been theoretically reported at visible frequencies [26]. With the development of emerging techniques, such as focused ion beam milling, holographic lithography, and quantum tailoring of large molecules, it seems likely that these designs can be successfully met.

IV. CONCLUSION

In conclusion, we discuss the quantum interference between Zeeman levels of atom in the structure containing LHM and ZIM. In free space, such atomic two-transition dipoles cannot interfere with each other, because they are orthogonal which means one is left rotated and the other is right rotated. However, decomposing them into the component normal to the surface and the component parallel to the surface in the anisotropic environment, they are equivalent to being parallel through suppressing the component normal to the surface and can interfere with each other. We design the structure to get strong quantum interference with suppressed decay rates by introducing two kinds of artificial materials, i.e., left-handed materials and zero-index metamaterials. Without the dissipation of LHM and ZIM, simple double-layer structure can approach the goal. In this structure, LHMs have been used to shift the position of strong quantum interference away from the interface due to the phase compensation and refocusing effect, while ZIM is used to suppress decay rates at that position, i.e., $\Gamma_{||} = 0.5\Gamma_0$ and $\Gamma_{\perp} = 0$ due to its special reflective behavior $r_{\mathrm{ZIM}}^{\mathrm{TM}} \to -1$.

When considering the dissipation of materials, the Fabry-Pérot cavity made of matched ZIM and LHM has been suggested. Here, the function of LHM is to avoid the influence of nonradiative decay related to the material's loss. Meanwhile, the special reflective behavior of ZIM can suppress decay strongly for perpendicular orientation of a dipole. Furthermore, we can approach anisotropy through the different characters of spontaneous decays between dipole component normal to the surface and that parallel to the surface. Within an appropriate parameter range, strong quantum interference with suppressed decay rates in the case of dissipation is achieved. As all decay rates are smaller than the vacuum decay rates accompanied with maximum quantum interference, the duration time of interference is increased.

ACKNOWLEDGMENTS

This work is supported in part by the National Natural Science Foundation of China (Grant No. 11274242), the Joint Fund of the National Natural Science Foundation of China and the China Academy of Engineering Physics (Grant No. U1330203), the National Key Basic Research Special Foundation of China (Grants No. 2011CB922203 and No. 2013CB632701), and the Fundamental Research Funds for the Central Universities.

[1] V. G. Arkhipkin and Y. I. Heller, Phys. Lett. A **98**, 12 (1983).
[2] M. O. Scully, S.-Y. Zhu, and A. Gavrielides, Phys. Rev. Lett. **62**, 2813 (1989).
[3] S. E. Harris, J. E. Field, and A. Imamoğlu, Phys. Rev. Lett. **64**, 1107 (1990).
[4] K. Hakuta, L. Marmet, and B. P. Stoicheff, Phys. Rev. Lett. **66**, 596 (1991).
[5] P. Zhou and S. Swain, Phys. Rev. Lett. **77**, 3995 (1996).
[6] C. H. Keitel, Phys. Rev. Lett. **83**, 1307 (1999).
[7] F.-l. Li and S.-Y. Zhu, Phys. Rev. A **59**, 2330 (1999).
[8] S.-Y. Zhu and M. O. Scully, Phys. Rev. Lett. **76**, 388 (1996).
[9] Z. Ficek and S. Swain, *Quantum Interference and Coherence: Theory and Experiments* (Springer, Berlin, 2005).
[10] M. O. Scully, *Quantum Optics* (Cambridge University Press, Cambridge, 1997).
[11] G. S. Agarwal, Phys. Rev. Lett. **84**, 5500 (2000).
[12] J.-P. Xu, L.-G. Wang, Y.-P. Yang, Q. Lin, and S.-Y. Zhu, Opt. Lett. **33**, 2005 (2008).
[13] G.-x. Li, F.-l. Li, and S.-y. Zhu, Phys. Rev. A **64**, 013819 (2001).
[14] G.-x. Li, J. Evers, and C. H. Keitel, Phys. Rev. B **80**, 045102 (2009).
[15] J.-P. Xu and Y.-P. Yang, Phys. Rev. A **81**, 013816 (2010).
[16] V. Yannopapas, E. Paspalakis, and N. V. Vitanov, Phys. Rev. Lett. **103**, 063602 (2009).
[17] X. Zeng, J. Xu, and Y. Yang, Phys. Rev. A **84**, 033834 (2011).

[18] Y. Yang, J. Xu, H. Chen, and S. Zhu, Phys. Rev. Lett. **100**, 043601 (2008).
[19] H.-R. Xia, C.-Y. Ye, and S.-Y. Zhu, Phys. Rev. Lett. **77**, 1032 (1996).
[20] L. Li, X. Wang, J. Yang, G. Lazarov, J. Qi, and A. M. Lyyra, Phys. Rev. Lett. **84**, 4016 (2000).
[21] M. V. Gurudev Dutt, J. Cheng, B. Li, X. Xu, X. Li, P. R. Berman, D. G. Steel, A. S. Bracker, D. Gammon, S. E. Economou, R.-B. Liu, and L. J. Sham, Phys. Rev. Lett. **94**, 227403 (2005).
[22] V. G. Veselago, Sov. Phys. Usp. **10**, 509 (1968).
[23] J. B. Pendry, Phys. Rev. Lett. **85**, 3966 (2000).
[24] S. A. Ramakrishna, Rep. Prog. Phys. **68**, 449 (2005).
[25] H. Chen, C. T. Chan, and P. Sheng, Nat. Mater. **9**, 387 (2010).
[26] S. P. Burgos, R. de Waele, A. Polman, and H. A. Atwater, Nat. Mater. **9**, 407 (2010).
[27] D. R. Smith, W. J. Padilla, D. C. Vier, S. C. Nemat-Nasser, and S. Schultz, Phys. Rev. Lett. **84**, 4184 (2000).
[28] S. Zhang, W. Fan, N. C. Panoiu, K. J. Malloy, R. M. Osgood, and S. R. J. Brueck, Phys. Rev. Lett. **95**, 137404 (2005).
[29] V. M. Shalaev, W. Cai, U. K. Chettiar, H.-K. Yuan, A. K. Sarychev, V. P. Drachev, and A. V. Kildishev, Opt. Lett. **30**, 3356 (2005).
[30] G. Dolling, C. Enkrich, M. Wegener, C. M. Soukoulis, and S. Linden, Science **312**, 892 (2006).
[31] G. Dolling, C. Enkrich, M. Wegener, C. M. Soukoulis, and S. Linden, Opt. Lett. **31**, 1800 (2006).
[32] J. Valentine, S. Zhang, T. Zentgraf, E. Ulin-Avila, D. A. Genov, G. Bartal, and X. Zhang, Nature **455**, 376 (2008).
[33] H. J. Lezec, J. A. Dionne, and H. A. Atwater, Science **316**, 430 (2007).
[34] G. Dolling, M. Wegener, C. M. Soukoulis, and S. Linden, Opt. Lett. **32**, 53 (2007).
[35] R. Liu, Q. Cheng, T. Hand, J. J. Mock, T. J. Cui, S. A. Cummer, and D. R. Smith, Phys. Rev. Lett. **100**, 023903 (2008).
[36] B. Edwards, A. Alù, M. E. Young, M. Silveirinha, and N. Engheta, Phys. Rev. Lett. **100**, 033903 (2008).
[37] B. Edwards, A. Alu, M. G. Silveirinha, and N. Engheta, J. Appl. Phys. **105**, 044905 (2009).
[38] L. Zhang, Y. Zhang, Y. Yang, and H. Chen, Phys. Rev. E. **83**, 046604 (2011).
[39] H.-t. Jiang, Z.-l. Wang, Y. Sun, Y.-h. Li, Y.-w. Zhang, H.-q. Li, and H. Chen, J. Appl. Phys. **109**, 073113 (2011).
[40] D.-H. Kwon and D. H. Werner, Opt. Express **15**, 9267 (2007).
[41] Ernst Jan R. Vesseur, T. Coenen, H. Caglayan, N. Engheta, and A. Polman, Phys. Rev. Lett. **110**, 013902 (2013).
[42] R. Maas, J. Parsons, N. Engheta, and A. Polman, Nat. Photonics **7**, 907 (2013).
[43] R. W. Ziolkowski, Phys. Rev. E. **70**, 046608 (2004).
[44] A. Alù, M. G. Silveirinha, A. Salandrino, and N. Engheta, Phys. Rev. B **75**, 155410 (2007).
[45] M. Silveirinha and N. Engheta, Phys. Rev. Lett. **97**, 157403 (2006).
[46] S. Enoch, G. Tayeb, P. Sabouroux, N. Guérin, and P. Vincent, Phys. Rev. Lett. **89**, 213902 (2002).
[47] V. C. Nguyen, L. Chen, and K. Halterman, Phys. Rev. Lett. **105**, 233908 (2010).
[48] X. Huang, Y. Lai, Z. H. Hang, H. Zheng, and C. T. Chan, Nat. Mater. **10**, 582 (2011).
[49] L.-G. Wang, Z.-G. Wang, J.-X. Zhang, and S.-Y. Zhu, Opt. Lett. **34**, 1510 (2009).
[50] F. Wang and C. T. Chan, Europhys. Lett. **99**, 67002 (2012).
[51] M. S. Tomaš, Phys. Rev. A **51**, 2545 (1995).
[52] M. Born, E. Wolf, and A. B. Bhatia, *Principles of Optics: Electromagnetic Theory of Propagation, Interference and Diffraction of Light* (Cambridge University Press, Cambridge, 1999).